

RESPONSE OF A TURBULENT BOUNDARY LAYER TO SUDDEN CHANGES IN WALL TEMPERATURE AND ROUGHNESS

Mila R. Avelino[†] and Atila P. Silva Freire
Mechanical Engineering Program (PEM/COPPE/UFRJ),
C.P. 68503, 21945-970 - Rio de Janeiro - Brazil.

[†]Also: Department of Mechanical Engineering (UERJ),
R. São Francisco Xavier, 524/5023A, 20550-013, Rio de Janeiro - Brazil.

Abstract. *The present work reports the dynamic and thermal behaviour of flows that develop over surfaces which show a sudden change in surface temperature and roughness. A particular interest of this study is to investigate any existing relationship between the error in origin for both the velocity (ε) and the temperature (ε_t) profiles, so that any analogy between the logarithmic laws for the velocity and the temperature profiles can be assessed. Then, by considering the validity of Coles's law of the wake for the outer part of the boundary layer, a robust algebraic equation for the estimation of Stanton number is proposed. Three different types of surfaces are considered here: two 'K' type of surfaces and one 'D' type of surface. The flow is made to pass from a cold smooth surface to a hot rough surface. Measurements are presented for the mean velocity and temperature profiles. Also, all global parameters that characterise the velocity and the temperature fields are presented. The results show that for surfaces of type 'K' the behaviour of ε and of ε_t are very similar; for surfaces of type 'D', however, their behaviour is quite different.*

Key words: *turbulence, thermal boundary layer, roughness, error in origin.*

1. INTRODUCTION

A classical means to enhance the heat transfer at a wall is to use surfaces that are not smooth but rough. Then, depending on the geometry of the roughness elements, the heat transfer can be altered at will. In fact, the problem of selecting surfaces that will furnish a determined heat transfer coefficient to a particular application is not a trivial one. A classical case of failure in the design of heat exchangers is the use of surfaces where the roughness elements are very close together so that well defined recirculating regions are formed in the grooves. In this situation, the trapped fluid may act as an insulator, dramatically decreasing the heat transfer rate. Thus, in this example, the rough surface has a detrimental effect on the desired flow properties.

In previous studies of flows over rough surfaces, different methods have been used to construct the roughness. The early studies have used sand grains glued on the surface. The more recent studies have preferred to machine protrusions with a well defined geometry. In the latter case, authors (see, e.g., Perry and Joubert(1963) Antonia and Luxton(1971,1972), Wood and Antonia,(1975)) have classified the rough surfaces into two distinct types of surfaces: 1) ‘*K*’ type rough surfaces and, 2) ‘*D*’ type rough surfaces. In cases where the nature of the roughness can be expressed with the help of a single length scale - the height of the protrusions, ‘*K*’ - the surface is termed of type ‘*K*’. Flows, on the other hand, which are apparently insensitive to the characteristic scale *K*, but depend on other global scale of the flow are termed ‘*D*’ type flows. This is the case, just mentioned above, when the roughness is geometrically characterised by a surface with a series of closely spaced grooves within which the flow generates stable vortical configurations.

Naturally, most of the studies on flows over rough surfaces have dealt so far with the velocity field. Indeed, the complexities caused by the roughness on the proper assessment of the flow properties are of such an order that, even today, after the advent of very sophisticated measuring techniques, much still remains to be understood about the problem. That is the reason why just a small number of works on the temperature field are available in literature. The result is that, for the evaluation of properties related to the thermal boundary layer, the standard approach is to resort to some analogy between the momentum and the heat transfer processes. For simple flow situations, such as flows in the completely developed regime, these approaches are seen to provide good results. For example, the classical result $C_f/2 = S_t$, where C_f is the skin-friction coefficient and S_t is the Stanton number, is a very good working expression extensively in the past.

The purpose of this work is to investigate both the velocity and the temperature fields of boundary layer flows that develop over surfaces with a sudden change in roughness. In the cases of interest to be studied here, a cold flow over a smooth surface is made to pass over a hot, rough surface. In this situation, it is not clear that a straight Reynolds analogy will work. Here we are specially interested in studying the validity of the two universal relations, the law of the wall and the law of the wake, for both, the velocity and the temperature fields.

For flows over a rough surface, we know that C_F and S_t cannot be evaluated directly through methods that resort to the gradient of the log-law because the effective origin of the boundary layer is not known a priori. This prompted some authors (e.g., Perry and Joubert(1963), Perry et al.(1985)) to develop detailed procedures for the determination of this effective origin that could be used to evaluate C_f directly from the angular coefficient of a “corrected” law of the wall.

In this work, the behaviour of the error in origin for the velocity and the temperature fields will be investigated for three types of rough surface. Then, any analogy between the velocity and the temperature fields will be assessed. To achieve that, the present work will investigate experimentally the characteristics of turbulent boundary layers that are subjected to a step change in surface roughness and temperature, with emphasis on the characterisation of the inner layer velocity and temperature profiles. Due to a pressing shortage of space, we will refrain from making any literature review on the subject. For that, the reader is referred to Guimarães et al.(1999).

Table 1: Geometry of the roughness elements.

Type	K (mm)	W (mm)	S (mm)	λ (mm)	W/K
I	4,77	15,88	15,88	31,76	3.33
II	4,77	31,76	15,88	47,64	6.66
III	6,35	15,88	4,76	20,64	2.5

2. EXPERIMENTAL APPARATUS AND PROCEDURE

The experiments were carried out in the high-turbulence wind tunnel sited at the Laboratory of Turbulence Mechanics of PEM/COPPE/UFRJ. The tunnel characteristics and its instrumentation are detailed described in Guimarães et al.(1999) and for this reason will not be repeated here.

The flow was subjected to a step change in roughness after travelling the first meter over the glass floor. Three types of rough surface were considered where the roughness elements consisted of equally spaced transversal rectangular slats. The dimensions of the roughness elements are shown in Table (1) where K denotes the height, S the length, W the gap, and λ the pitch. In constructing the surface, extreme care was taken to keep the first roughness element always depressed below the smooth surface, its crest kept aligned with the smooth glass wall surface.

The smooth surface was also followed by a step change in temperature. The rough surface was heated up to 102.2 ± 1.5 °C. The measurements were performed for values of the free-stream velocity of 3.12 m/s; the free stream level of turbulence was about 2%.

3. THEORY

Before we move on, let us first briefly review the theory presented in Guimarães et al.(1999). For more details, see the original work.

For any kind of rough surface, it is possible to write

$$\frac{u}{u_\tau} = \frac{1}{\kappa} \ln \frac{(y_T + \varepsilon)u_\tau}{\nu} + A - \frac{\Delta u}{u_\tau}, \quad (1)$$

where,

$$\frac{\Delta u}{u_\tau} = \frac{1}{\kappa} \ln \frac{\varepsilon u_\tau}{\nu} + C_i, \quad (2)$$

and u_τ is the friction velocity, y_T is the vertical distance measured from the crest of the roughness elements, ε is the error in origin, $\kappa = 0.4$, $A = 5.0$, and $C_i, i = K, D$; is a constant characteristic of the roughness.

The above equations, although of a universal character, have the inconvenience of needing two unknown parameters for their definition, the skin-friction velocity, u_τ , and the error in origin, ε .

Equations 1 and 2 can be extended to the outer part of the flow by considering Coles's wake hypothesis to hold. Thus, the law of the wall can be re-written as

$$\frac{u}{u_\tau} = \frac{1}{\kappa} \ln \frac{(y_T + \varepsilon)u_\tau}{\nu} + A - \frac{\Delta u}{u_\tau} + \frac{\Pi}{\kappa} W\left(\frac{y}{\delta}\right), \quad (3)$$

where W is a universal function of y/δ and Π is a parameter dependent on the upstream shear stress and pressure distribution.

Substitution of $(y, u)=(\delta, U_\infty)$ into equation 3 furnishes

$$\frac{U_\infty}{u_\tau} = \frac{1}{\varkappa} \ln \frac{\delta + \varepsilon}{\varepsilon} + A - C_i + \frac{2\Pi}{\varkappa}. \quad (4)$$

This simple algebraic equation furnishes values of $C_f (= 2 u_\tau^2/U_\infty^2)$ for known values of U_∞ , δ and ε .

To extend expressions 1 and 2 to the temperature turbulent boundary layer we use some simple analogy arguments. The similarity in transfer processes for turbulent flows suggests that (for more details see Guimarães et al.(1999))

$$\frac{T_w - t}{t_\tau} = \frac{1}{\varkappa_t} \ln P_r \frac{(y_T + \varepsilon_t)u_\tau}{\nu} + B - \frac{\Delta t}{t_\tau}, \quad (5)$$

where,

$$\frac{\Delta t}{t_\tau} = \frac{1}{\varkappa_t} \ln P_r \frac{\varepsilon_t u_\tau}{\nu} + D_i, \quad (6)$$

and $D_i, i = K, D$; is a constant characteristic of the roughness.

Equations 5 and 6 are the law of the wall formulation for flows over rough surfaces with transfer of heat at the wall.

To describe the temperature profile in the defect region of the boundary layer, we may consider that Coles's wake hypothesis also holds for the temperature field so that equation 3 may be re-written as

$$\frac{T_w - t}{t_\tau} = \frac{1}{\varkappa_t} \ln P_r \frac{(y_T + \varepsilon_t)u_\tau}{\nu} + B - \frac{\Delta t}{t_\tau} + \frac{\Pi_t}{\varkappa_t} W\left(\frac{y}{\delta_t}\right), \quad (7)$$

where the wake profile Π_t should, in principle, be a function of the enthalpy thickness.

This equation provides a representation for the temperature field which can be allowed to sustain a different state of development from the velocity field. As a result, Stanton number can be evaluated independently from the skin-friction through an independent algebraic equation. To find this equation, we substitute $(y, t)=(\delta_t, T_\infty)$ into equation 7 to get

$$\frac{T_w - T_\infty}{t_\tau} = \frac{1}{\varkappa_t} \ln P_r \frac{(\delta_t + \varepsilon_t)}{\varepsilon_t} + B - D_i + \frac{2\Pi_t}{\varkappa_t}. \quad (8)$$

This algebraic equation can now be used to find Stanton number as a function of T_∞ , δ_t and ε .

4. EXPERIMENTS

4.1. Velocity profile data

The measured velocity profiles for the three different flow configurations are shown in Figures 1 to 3. It is clear from these Figures that the would be logarithmic regions of the flow have suffered a slight deformation to the left side. In fact, as we shall see, a

very popular method to find ε is based on a procedure to restore the lower portion of the velocity profile to a logarithmic profile.

The global parameters of the velocity boundary layers are shown in Figures 4 to 6, where δ denotes the boundary layer thickness, δ^* the displacement thickness and θ is the momentum thickness. Of particular note are the results for the Clauser Factor, G (see definition in Ligrani et al.(1983)). This parameter indicates the state of equilibrium of the boundary layer. For the values found here, the boundary layer is in a self-preserving state. Please, note that the evaluation of G depends on the knowledge of $C_f/2$ which, in principle, is not known at the moment. The determination of $C_f/2$ is explained in the following.

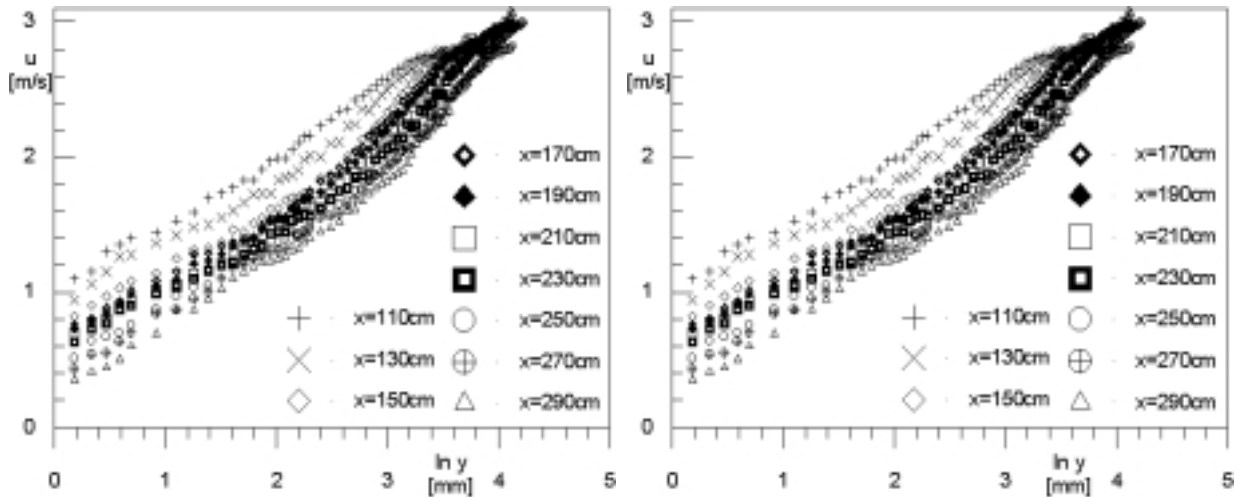


Figure 1: Velocity profiles. Roughness of type I.

Figure 2: Velocity profiles. Roughness of type II.

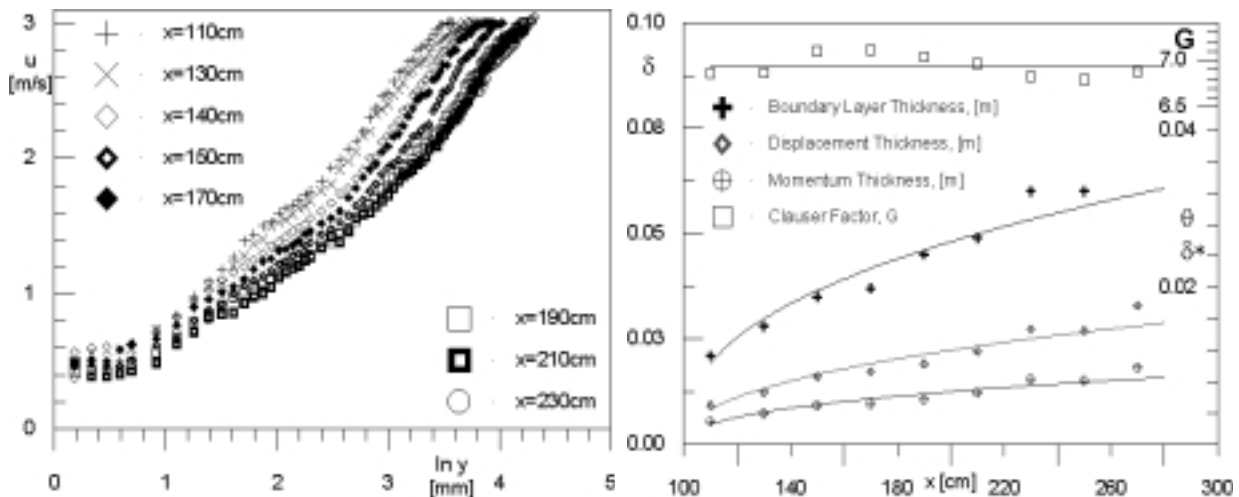


Figure 3: Velocity profiles. Roughness of type III.

Figure 4: Global parameters. Roughness of type I.

The error in origin, ε , was estimated by four different procedures. In fact, the procedures of Perry and Joubert(1963) and of Perry et al.(1987) are the most rigorous that can

be found in literature so that the data resulting from them must be seen as very reliable. The procedures of Thompson(1978) and of Bandyopadhyay(1987) are very simplified so that the values of ε obtained through them must be seen just as a first approximation.

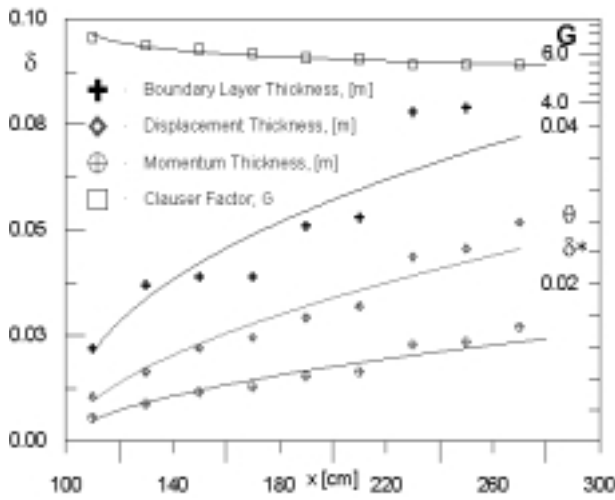


Figure 5: Global parameters. Roughness of type II.

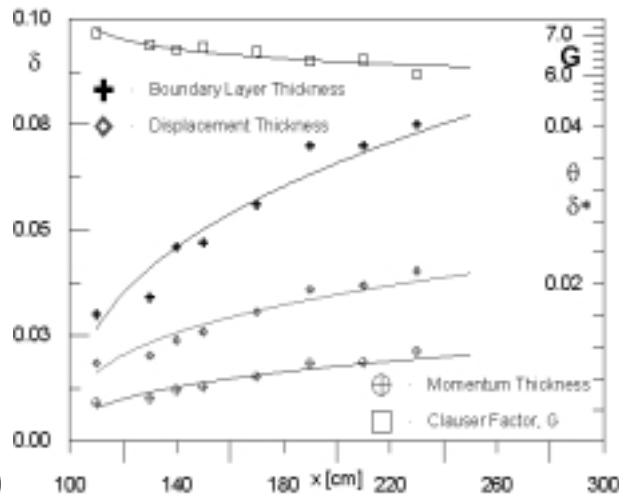


Figure 6: Global parameters. Roughness of type III.

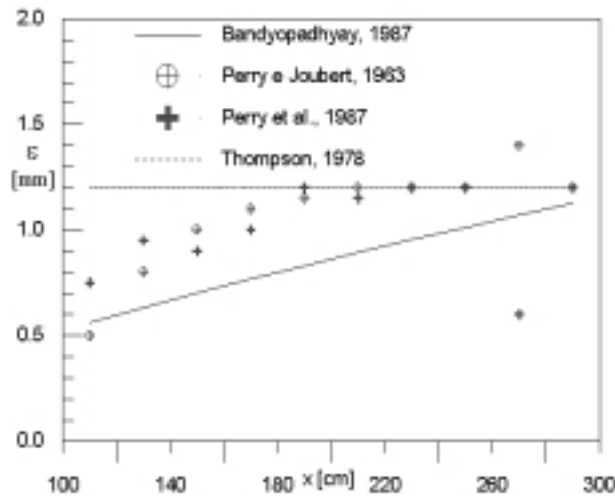


Figure 7: Error in origin. Roughness of type I.

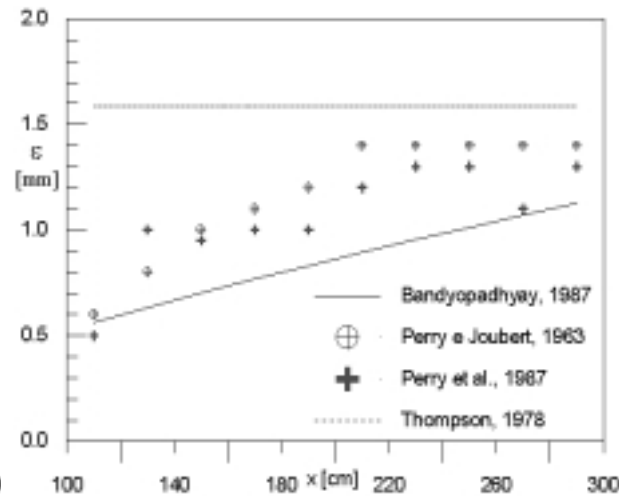


Figure 8: Error in origin. Roughness of type II.

In the Perry and Joubert(1963) method, arbitrary values of ε are added to the wall distance and a straight line is fitted to the log-law region. The value of ε that furnishes the best discriminated logarithmic region is then considered to be the correct value for the error in origin. The method of Perry et al(1987) is more sophisticated, resorting to a cross plot of ε vs $2\Pi/\varkappa$, where Π stands for Coles's wake profile.

The ε results for the rough surfaces of all types, I, II and III, are presented in Figures 7 to 9. Considering the high degree of difficulty involved in finding these results, and the very good agreement between the predictions based on the two more reliable procedures, we

may say that the results of ε and consequently of C_f are very consistent and representative of the flow.

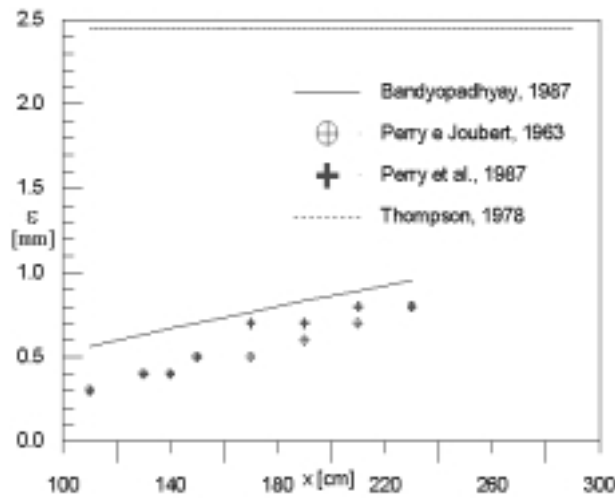


Figure 9: Error in origin. Roughness of type III.

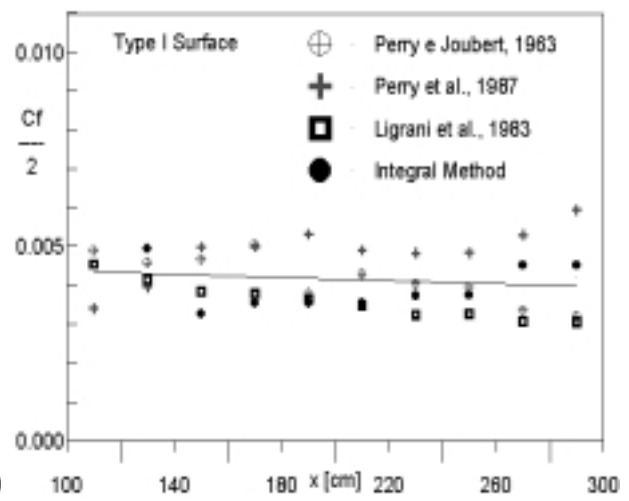


Figure 10: Skin friction coefficient.

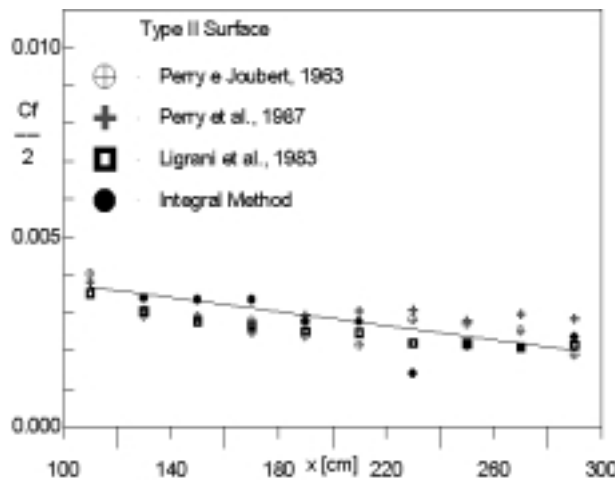


Figure 11: Skin friction coefficient.

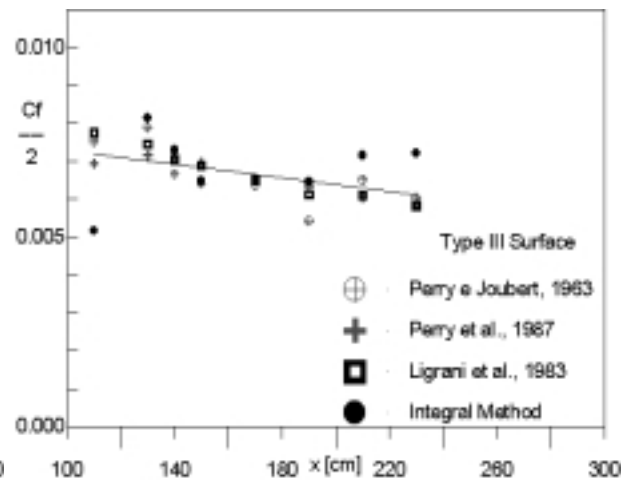


Figure 12: Skin friction coefficient.

The values of C_f obtained through the two velocity gradient methods are shown in Figures 10 to 12. They are also compared with two integral methods: i) the classical method that makes use of von Karman's integral momentum equation, and ii) another method based on an empirical expression advanced by Ligrani et al.(1983).

4.2. Temperature profile data

The measured temperature profiles for the three different flow configurations are shown in Figures 13 to 15. Much in the same way as with the velocity profiles, the temperature profiles are also observed to present a left shift. However, since close to the point of change in surface nature the thermal boundary layer is still in its initial state of development, the logarithmic region cannot be clearly seen in the first stations.

In any case, Figures 13 to 15 suggest that all the procedures advanced for the evaluation of ε and of C_f can be extended to the temperature profile for the evaluation of ε_t and of S_t . Then, a straight extension of the methods of Perry and Joubert(1963) and of Perry et al.(1987) to the temperature profiles yields Figures 16 to 18.

Figures 16 and 17 represent the flow over surfaces with roughness elements of types I and II. We have seen before that these surfaces are of type ‘K’ and that therefore ε should have a relatively high rate of growth. The experiments, however, show that ε_t always grows faster than ε . In all flow situations the error in origin for the temperature profiles was always found to be superior to the error in origin for the velocity profiles. This difference is particularly marked for the surface of type III, of type ‘D’.

Having found ε and ε_t , we can now use the gradient of the log-law to determine S_t ; this can be made through equations 1 and 5. The results are shown in Figures 19 to 21. These Figures also include results calculated with equation 8.

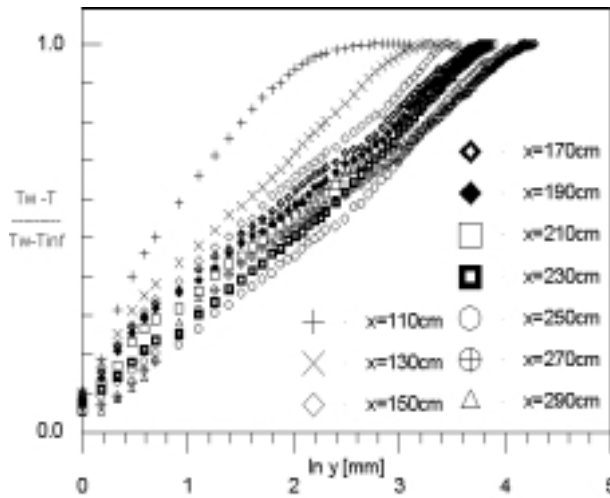


Figure 13: Temperature profiles. Roughness of type I.

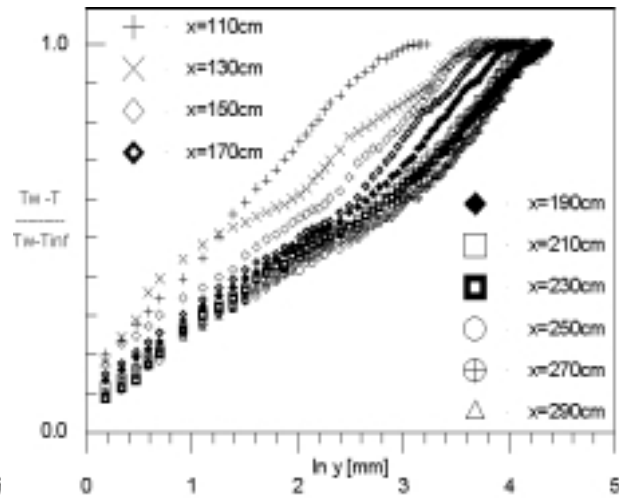


Figure 14: Temperature profiles. Roughness of type II.

5. FINAL REMARKS

The calculated values of ε and of ε_t were obtained through the methods of Perry and Joubert(1963) and of Perry et al.(1987). In the first method, by systematically adding an arbitrary value to the distance from the top of the roughness elements, a least square procedure was built to furnish the best discriminated straight line fit. The second method uses the universal wake profile of Coles and resorts to a cross plot of ε vs $2\Pi/\varkappa$.

In previous works, some authors (see, e.g., Guimarães et al.(1999)) have expected, on asymptotic grounds, that the values of ε and of ε_t would be very close. Here, we have shown that this appears to be the case for surfaces of the type ‘K’; for surfaces of type ‘D’ the results differed appreciably.

Finding the error in origin has always been a difficult problem that has plagued many authors. Here we have made for, perhaps, the first time in literature, a detailed comparison between ε and ε_t for three different types of surface. Since the main objective of this work has been to assess the usefulness of equations 4 and 8, we have presented

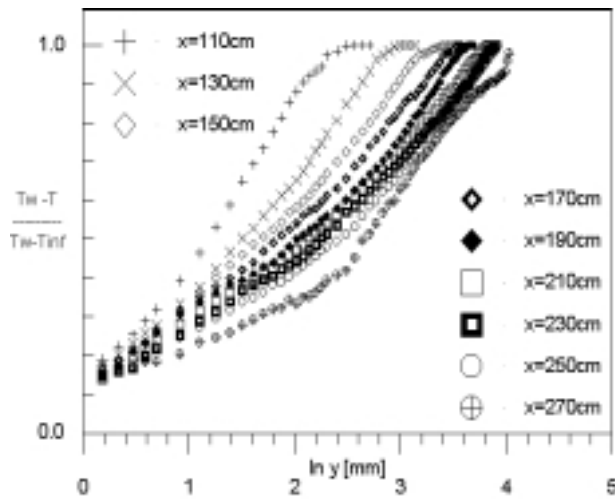


Figure 15: Temperature profiles. Roughness of type III.

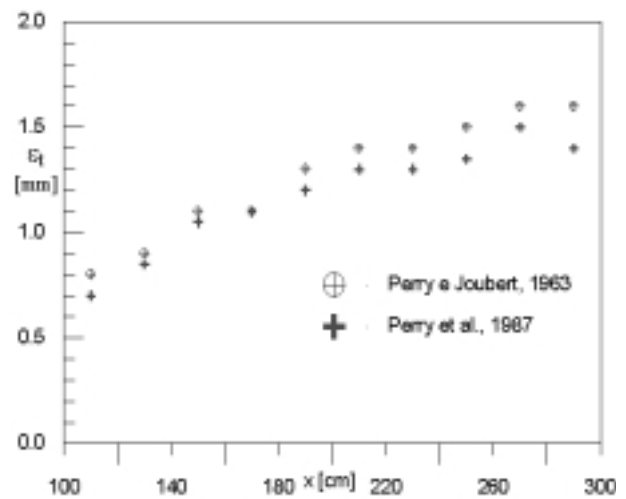


Figure 16: Error in origin, temperature.

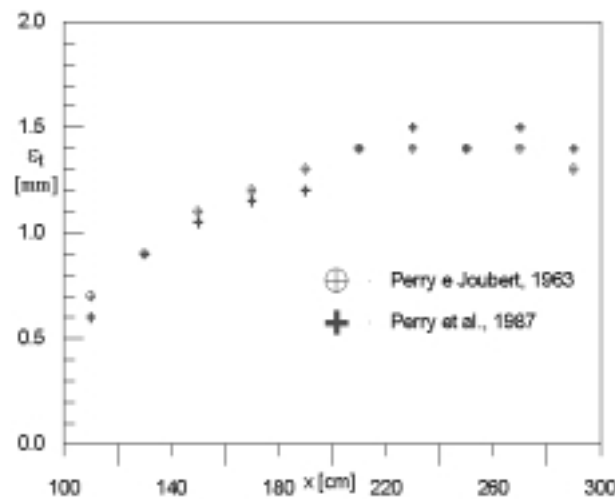


Figure 17: Error in origin, temperature.

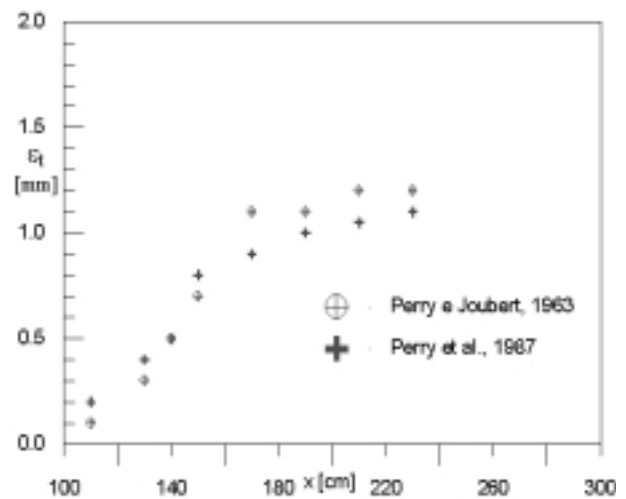


Figure 18: Error in origin, temperature.

only mean velocity and temperature data. Measurements of turbulent quantities and a further processing of the available data will be presented elsewhere.

In completion to the work of Guimarães et al.(1999), this work has shown that a working relationship between the rates of growth for the error in origin for the velocity and the temperature profiles can be established. This is a very important matter for it allows Stanton number to be evaluated directly from a proper equation which takes into account the different states of development of the velocity and the temperature boundary layers.

Acknowledgement. The present work was financially supported by the Brazilian National Research Council – CNPq – through grant No 350183/93-7.

REFERENCES

Antonia, R.A. and Luxton, R.E., 1971, *J. Fluid Mech.*, vol. 48, pp. 721–761.

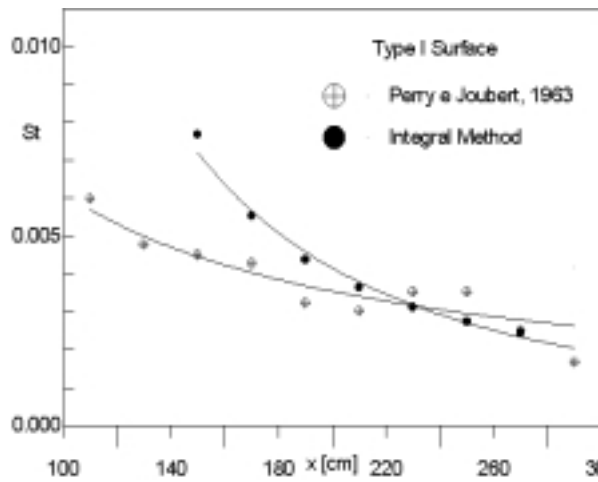


Figure 19: Stanton numbers.

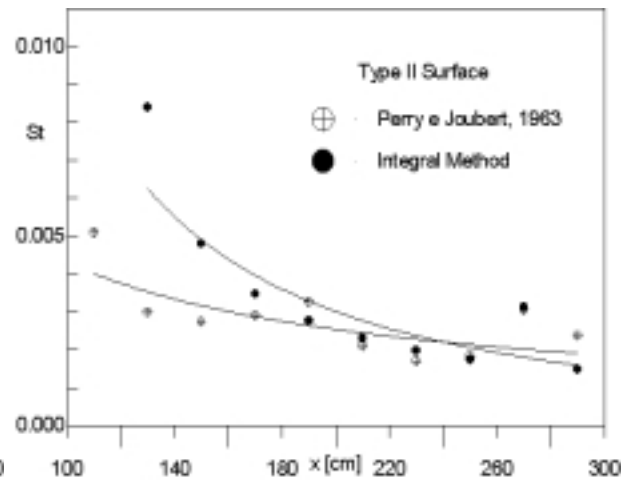


Figure 20: Stanton numbers.

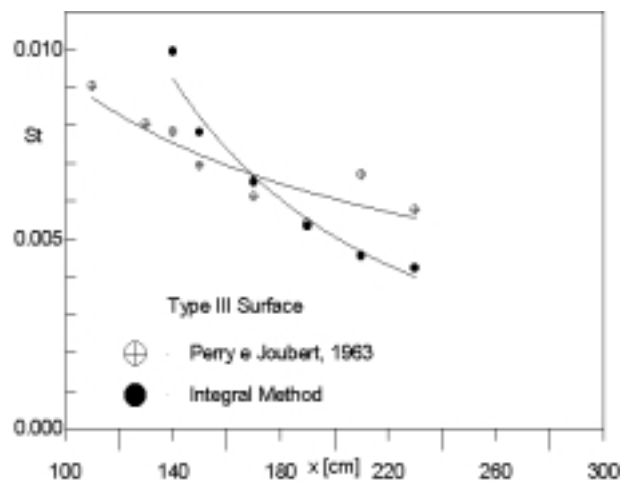


Figure 21: Stanton numbers.

Antonia, R.A. and Luxton, R.E., 1972, *J. Fluid Mech.*, vol. 53, pp. 737-757.

Bandyopadhyay, P.R., 1987, *J. Fluid Mech.*, vol. 180, pp. 231-266.

Guimarães, J.H.D., Santos Jr., S.J.F., Su, J., Silva Freire, A.P., 1999, Proc. IMECE99, November 12-14, Tennessee, USA.

Ligrani, P. M., Moffat, R. J. and Kays, W. M., 1983, *J. Fluids Engineering*, vol. 105, pp. 146-153.

Perry, A. E. and Joubert, P. N., 1963, *J. Fluid Mechanics*, vol. 17, pp. 193-211.

Perry, A. E., Lim, K. L. and Henbest, S. M., 1987, *J. Fluid Mech.*, vol. 177, pp. 437-466.

Thompson, R.S., 1978, *J. Appl. Meteorol.*, vol. 17, pp. 1402-1403.

Wood, D.H. and Antonia, R.A., 1975, *J. Applied Mech.*, vol. 53, pp. 591-596.